Cite this article
Arfaoui A, Naili H, Loulizi A and Siala A (2025)
Juncus fibres' treatment for use in stone matrix asphalt to improve its rutting resistance.
Proceedings of the Institution of Civil Engineers – Construction Materials **178(6)**: 322–331,
https://doi.org/10.1680/jcoma.24.00100

Research Article
Paper 2400100
Received 11/10/2024; Accepted 23/07/2025

Construction Materials

Juncus fibres' treatment for use in stone matrix asphalt to improve its rutting resistance

Amani Arfaoui
LR11ES16 Laboratory of Materials, Optimization, and Environment for Sustainability, National Engineering School of Tunis, Tunis El Manar University, Tunis, Tunisia (Orcid:0009-0002-4079-2199) (corresponding author: amani.arfaoui@enit.utm.tn)

Houcem Naili
Laboratory of Civil Engineering, National Engineering School, Tunis El Manar University, Tunis, Tunisia

Amara Loulizi
LR11ES16 Laboratory of Materials, Optimization, and Environment for Sustainability, National Engineering School of Tunis, Tunis El Manar University, Tunis, Tunisia (Orcid:0000-0003-1542-0086)

Ahmed Siala
Military Research Center, Tunis, Tunisia

This study investigated the effect of cellulose fibres extracted from Juncus plant stems on the rutting resistance of stone matrix asphalt (SMA). Replacing commonly used synthetic fibres with natural, locally available ones emerges as a sustainable solution, particularly given the growing demand for eco-friendly construction materials. Six chemical extraction treatments were tested, with alkalinisation at 98°C for 1 h in an 8% sodium hydroxide solution, followed by 1 h at ambient temperature in a 40% sodium hypochlorite solution, resulting in an optimal cellulose content of 64%. The extracted fibres were incorporated into SMA mixtures to assess their impact on performance. After determining the optimal asphalt content (OAC) through Marshall tests, two mixtures were selected: 6.2% OAC for SMA without fibres and 6.5% with 0.4% Juncus fibres. Performance was evaluated through Duriez compressive strength tests (18°C), gyratory shear compaction (155°C), and rutting wheel tests (60°C). Compared with the control mix, the compressive strength of the fibre-reinforced SMA was found to be 1.7 times higher, achieving 1% lower void content at 200 shear gyrations and 2.8 mm lower rutting depth at 30,000 wheel cycles. These findings demonstrate that Juncus fibres enhance SMA's mechanical properties, contributing to more sustainable roadway infrastructure.

Keywords: alkalisation/cellulose/construction/fibre-reinforcement/juncus fibres/organic/pavement design/rutting/stone matrix asphalt/sustainability

Notation

G_{ca}	bulk specific gravity of the coarse aggregate
G_{mb}	measure of bulk density
G_{mm}	measured maximum theoretical specific gravity of the mixture
G_{sb}	bulk specific gravity of the aggregates
P_{ca}	percentage coarse aggregate in the total mixture
P_s	percentage of aggregates in the mix
VCA_{DRC}	measure of voids in dry-rodded coarse aggregates
VCA_{mix}	measure of voids in the coarse aggregate of the entire mixture
VFA	measure of voids filled with asphalt
VMA	measure of voids in mineral aggregates
VTM	measure of voids in the total mixture
Y_s	unit weight of coarse aggregate in the dry-rodded condition
Y_w	unit weight of the water

1. Introduction and background

Rutting is a form of deterioration in a hot mix asphalt (HMA) surface layer, which is divided into three main types. Structural rutting affects the entire pavement structure due to a weak or water-saturated subgrade. Densification rutting occurs early in the pavement's life due to inadequate initial compaction, and flow rutting results from plastic deformation in HMA layers without volume change. This study focuses on flow rutting, which is identified by a depression near the centre of the wheel path, often with raised sides, causing major safety concerns, including steering difficulties and hydroplaning when water fills the ruts. Although the exact mechanism behind rutting is still being researched (Simms *et al*., 2020), it is agreed that HMA with low shear strength and/or low total voids is more prone to this deterioration. The low shear strength in HMA can be attributed to factors such as using a soft asphalt with high thermal susceptibility, high asphalt content, high mineral filler content, and improper shape and texture of aggregate particles. External factors such as high temperature, repeated heavy truck loadings, and slow-moving vehicles significantly accelerate rutting. Unfortunately, these factors are worsening, especially in developing countries that are expanding their road networks without effectively regulating overloaded trucks. In addition, climate change is increasing both average and extreme temperatures worldwide.

Developed countries have adopted stone matrix asphalt (SMA) over recent decades to minimise flow rutting (Blazejowski, 2011). SMA is a gap-graded HMA mixture that relies on stone-on-stone contact for strength and a rich bitumen paste for durability (NAPA, 2002). The SMA skeleton comprises a high proportion of coarse aggregates (60%–80% by weight) that repose against each other and interlock with each other. The matrix contains filler, fine aggregates, bitumen, and a stabilising agent. SMA was developed in Europe from the 1960s to resist rutting and studded tyre wear, while the interest in this type of mixture in the USA was sparked by the strong recommendation of the participants in the 1990 European Asphalt Study Tour (Brown *et al*., 1997a; NCHRP, 1999). By 2018, at least 18 US state highway agencies were using SMA regularly (Yin and West, 2018). Nevertheless, SMA is more expensive than conventional dense-graded mixtures due to higher asphalt contents, the need for stronger aggregates and polymer-modified bitumen, and the inclusion of stabilising fibres. This higher production cost is generally offset by better performance and longer service life (Brown *et al*., 1997b). However, this concept of life cycle cost analysis is seldom used in developing countries because most of these countries take loans and deal with institutions to improve the balance of their payments to build roads. Therefore, to minimise these loans and debts, their decision-makers constantly look for the lowest bid and not necessarily the most cost-effective one. In addition, highway agencies in these countries have been using job-mix formulas available to them for more than 50 years and are reluctant to make any new changes. For these reasons, this research aimed to formulate an SMA mixture using domestic materials and equipment, following recommendations from Europe, Asia, and the USA, adapted to local constraints. The main requirement from the country's highway agency dealing with HMA was to use the same ingredients used in conventional dense-graded mixtures (local limestone quarries for aggregates and imported 35/50 penetration-grade asphalt), and for any other material needed for the formulation to be found domestically.

A key SMA component is a stabiliser, also known as a drainage inhibitor. Due to its elevated binder content, there is potential for the binder to bleed down during the mixing, transport, or compaction of the mixture, a phenomenon called draindown. This issue is typically resolved using cellulose, mineral, or synthetic fibres (Blazejowski, 2011). Since cellulose fibres are not commercially available in the country and need to be imported, it was decided to extract them from existing widespread domestic plants. Previous research by national scientists (including one of the co-authors) successfully extracted cellulose from Juncus, a plant in the Juncaceae family, for use with cementitious composites (El Ghali *et al*., 2012; Omrani *et al*., 2020).

Therefore, the first task of this study was to develop a cost-effective method for extracting cellulose from Juncus stems. These fibres were then used in SMA formulation, marking the first known application of Juncus fibres in SMA production.

As discussed earlier, the use of cellulose fibres in SMA mixtures is to reduce their draindown susceptibility. Few research efforts have looked at whether these cellulose fibres influence resistance to flow rutting. For this reason, the researchers formulated two SMA mixes: one without fibres and one including these fibres to assess their effect on SMA resistance to permanent deformation. The only study found by the authors that investigated the effect of mineral and cellulose fibres on improving the rutting performance of SMA mixtures is that of Mokhtari and Nejad (2012). They used the dynamic creep test as an indicator of performance, and they found that the flow number of the SMA mix incorporating cellulose is about three times that of the mixture without fibres. Other studies evaluated the effect of different types of fibres on SMA rutting resistance, including that of Brown *et al*. (1997a), Raghuram and Chowdary (2013) and Jasni *et al*. (2020).

2. Materials' characterisation and experimental programme for SMA

2.1 Materials

The formulated SMA mixtures were produced using local limestone aggregates and filler and imported 35/50 penetration-grade bitumen. Except for the filler and the cellulose fibres, the ingredients are commonly used in the country's road network for dense-graded asphalt.

Two crushed quarried aggregate classes were used: 0/4 mm (the numbers represent the lower and upper sizes in mm) fine aggregates and 8/14 mm coarse aggregates. The limestone filler, mainly composed of calcium carbonate ($CaCO_3$), had a particle size below 80 μm and a specific gravity of 2.740. Figure 1 presents the gradation curves for all aggregate classes and the filler. Standard characterisation tests were performed following French specifications to determine their physical properties. Table 1 shows that the results met the local highway agency's specifications for dense-graded HMA. However, the Los Angeles abrasion value, critical for SMA production, barely met the required specifications for dense-graded mixtures.

The bitumen used was 35/50 based on the penetration-grading system, following conventional tests conducted according to French standards (Table 2). In addition, tests performed abroad using the American Association of State Highways and Transportation Officials (AASHTO, 2023) standard for performance-graded asphalt binders (Superpave) classified the bitumen as PG 64-10. The result was confirmed during the study by one of the co-authors (Ben Dhia *et al*., 2024).

2.2 Treatment of Juncus fibres

Juncus is a plant commonly found throughout the country, especially in wet areas, and grows in various environments. Its stems, averaging about 125 cm long and 3.3 mm diameter, contain interconnected cellulose fibres around the periphery, while the interior

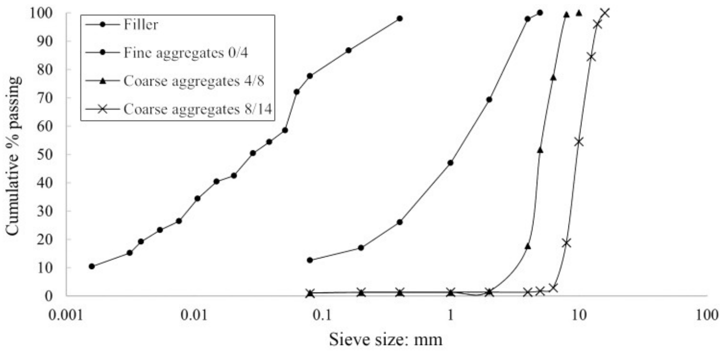

Figure 1. Gradation curves for all aggregates and filler material

Table 1. Results of the aggregates' characterisation tests

Aggregate class	0/4	4/8	8/14	Specifications
Test				
Micro-Deval test: % (AFNOR, 2011)	—	—	15	<20
LA test: % (AFNOR, 2020)	—	—	30	<30
Sand equivalent: % (AFNOR, 2015c)	76.6	—	—	>50
Absorption: % (AFNOR, 2001)	—	0.7	1.0	<2
Flat and elongated particles: % (AFNOR, 2012)	—	14.4	6	<25
Specific gravity (AFNOR, 2001)	2.730	2.650	2.650	2.5–3

Table 2. Results of the bitumen penetration-grading classification tests

Property	Value	Specifications
Needle penetration: 1/10 mm (AFNOR, 2015a)	45	35–50
Softening point test: °C (AFNOR, 2015b)	52	50–58
Flash and fire point: °C (ESC, 2017)	250	>240
% Loss after rolling thin film oven rest RTFOT: % (ESC, 2014)	0	<0.01
Penetration test after RTFOT: % original value (AFNOR, 2015a)	67	>45
Softening point test after RTFOT: °C (AFNOR, 2015b)	56	>52

fibres are separated by empty alveolate cells. Scanning electron microscope images show that the structure of Juncus stems is unsuitable for reinforcement, as lignin and hemicellulose in the alveolar cells must be removed to extract the cellulose fibres.

As Naili *et al*. (2017) suggested, cellulose extraction from Juncus stems can be achieved using various simple, cost-effective treatments. This study employed alkalisation treatment with two different concentrations of sodium hydroxide (NaOH) (4% and 8%), either with or without sodium hypochlorite (NaOCl), a delignification agent, along with chlorine bleaching (B) to eliminate lignin compounds. The following treatments were applied:

(*a*) Ambient process (A): Juncus stems are cut into 10 ± 1 cm pieces and placed in a beaker filled with an aqueous solution of sodium hydroxide at concentrations of 4% (A4) or 8% (A8) by mass of water for 48 h at room temperature. Fibres were then rinsed with tap water and dried at room temperature.

(*b*) Hot process (H): Juncus stems are cut into pieces approximately 10 ± 1 cm long and placed in a filled beaker for 2 h with a 4% (H4) concentration of sodium hydroxide and 1 h with an 8% (H8) concentration of sodium hydroxide at 98°C ± 2°C, followed or not by treatment with sodium hypochlorite at 40% per litre of water for 1 h. After each hot treatment, the treated fibres are rinsed with tap water and dried at room temperature.

This study evaluated six treatments. Figure 2 shows photos of the extracted fibres for each treatment.

2.2.1 Chemical composition of untreated and treated fibres

The chemical composition of untreated (U) and treated fibres was analysed using the protocols outlined by the Technical Association of the Pulp and Paper Industry (TAPPI). Treatment yield was calculated as the ratio of the final mass to the initial mass, multiplied by 100%.

TAPPI T211 om-07 (TAPPI, 2007) was used for ash content, where fibres were heated at 525°C for 4 h, and the percentage of ash was calculated as the ratio of ash mass to the initial mass

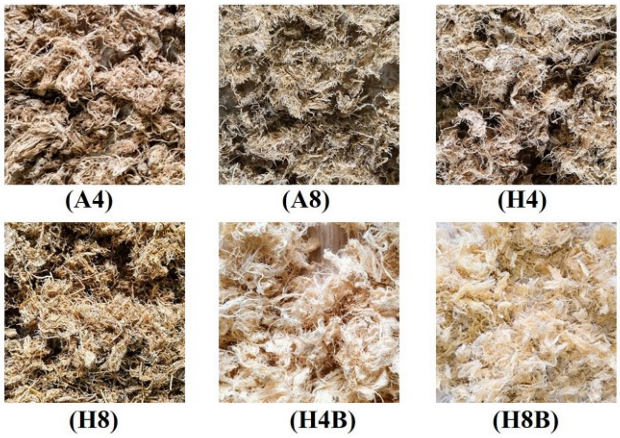

Figure 2. Extracted fibres after the chemical treatments

multiplied by 100%. Lignin content was determined using TAPPI protocols T222 om-06 (TAPPI, 2006) and um 250-91 (TAPPI, 1991), and cellulose content was measured using TAPPI T203 cm-99 (TAPPI, 1999). Holocellulose content was determined following Wise *et al*. (1946), and hemicellulose content was obtained by subtracting the cellulose content from holocellulose.

The measured ash content for the untreated fibres was found to be around 5%, whereas the treated fibres were around 3%. Figure 3(a) shows how yield and cellulose content were influenced by temperature, sodium hydroxide concentration, and sodium hypochlorite use. Comparing the H4 to A4 and H8 to A8 treatments, the yield decreased by 24% and 10%, respectively, whereas the cellulose content increased by 14% and 18%, respectively. Comparing A8 to A4 and H8 to H4, the yield decreased by 20% and 5%, respectively, whereas the cellulose content increased by 5% and 8%, respectively. In H4B to H4 and H8B to H8, the yield decreased by 8%, whereas the cellulose content increased by 27% and 21%, respectively. These findings indicate that higher temperatures, sodium hydroxide content, and sodium hypochlorite bleaching decrease yield but increase cellulose content, with H8B providing the best cellulose content (64%) and lowest yield (33%). Figure 3(b) shows non-cellulosic compounds, with the lowest hemicellulose (20%) and lignin (6%) in H8B-treated fibres. The results confirm that the H8B treatment is the most effective.

2.2.2 Physical properties of untreated and treated fibres

Cross-section diameter and density were measured for both untreated and treated fibres. A digital microscope was used to take 200 diameter measurements along the longitudinal axis of each fibre. Descriptive statistics were applied to the data, and box and whisker plots were created to compare untreated and treated fibres (Figure 4). All treatments reduced the fibre diameter, with the untreated fibres showing a minimum diameter of 241 mm, which is significantly larger than the maximum diameter of any treated fibre (131 mm for A4-treated fibres). The variability in diameter measurements also decreased with treatment, with the range shrinking from 97 mm for untreated fibres to 47 mm for H8-treated fibres. Except for the H4B treatment, the median diameter decreased

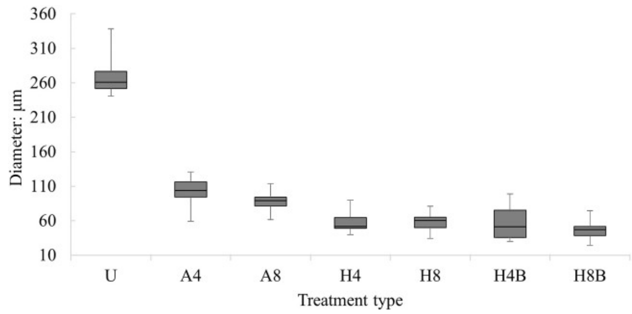

Figure 4. Box and whisker plots for the measured fibres' cross-sectional diameter

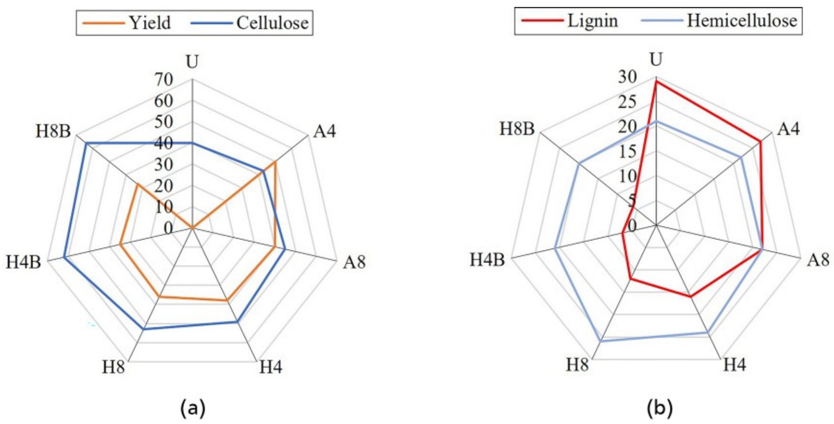

Figure 3. Chemical composition results: (a) yield and cellulose content; (b) lignin and hemicellulose contents

as treatment temperature, sodium hydroxide concentration, and bleaching increased. The lowest median diameter (47 mm) was observed in H8B-treated fibres.

Density was measured according to French standard NFT 20 053 (AFNOR, 1985). This involved placing a specific quantity of fibres into a pycnometer filled with carbon tetrachloride (CCl_4) and calculating the density using the measured masses of the empty pycnometer, the measured mass of the pycnometer filled with carbon tetrachloride, the measured mass of the pycnometer containing the fibres, the measured mass of the pycnometer filled with carbon tetrachloride and containing the fibres, and the density of carbon tetrachloride (1.584 g/cm^3). Figure 5 shows that the untreated fibres had an average density of 0.395 g/cm^3, which increased to about 0.956 g/cm^3 for the ambient-treated fibres and 1.154 g/cm^3 for the hot-treated fibres. The highest average density, 1.197 g/cm^3, was recorded for H8B-treated fibres. These results confirmed that the treatments successfully defibrated, delignified, and extracted cellulose fibres without damaging them.

Based on these chemical and physical tests, the H8B treatment was selected for cellulose extraction, as it yielded the highest cellulose content and density. This 2 h, cost-effective method produced the fibres used in the SMA formulation discussed in Section 2.3 Experimental programme.

2.3 Experimental programme

The experimental programme (Figure 6) began with formulating two SMA mixtures: one without and another incorporating cellulose fibres extracted from the Juncus plant. A crucial step in designing the SMA mixture was establishing a gradation curve for the aggregate mixture based on the nominal maximum aggregate size (NMAS). Binder content was then adjusted using Marshall tests, evaluating three asphalt contents: 5.9%, 6.2%, and 6.5%, following the National Centre for Asphalt Technology specifications for designing SMA by way of the Marshall method (Brown *et al*., 1998). The main criterion for two designs to pass the requirements is that the voids in the total mixture (VTM) should be as close as possible to 4%. For the SMA mixture with fibres, the fibre content was also changed depending on the obtained Marshall results. Different percentages of fibres were used, ranging from 0.1% to 0.5%. The incorporation of fibres followed the dry process method, where the fibres were cut into small pieces (approximately 5 mm long) and added directly to the aggregate mixture before adding bitumen. The two SMA mixtures with and without fibres that met the VTM criterion were then evaluated using the Duriez, gyratory shear compactor (GSC), and rutting wheel tests. Details of these tests are presented below.

2.3.1 Marshall test

The Marshall test followed the European standard EN 12697-34 (ESC, 2020a). For each tested mix, five specimens were prepared using 100 mm-diameter moulds preheated for 4 h at 155°C and compacted using 50 hammer blows on each side. Three specimens were used to determine the stability and flow values at 60°C, and two were used to measure the G_{mb}. Volumetric properties of the mix were then calculated, including VTM (Equation 1), VMA (Equation 2), VFA (Equation 3), VCA_{DRC} (Equation 4), and VCA_{mix} (Equation 5).

1. $$VTM = 100 \times \left(1 - \frac{G_{mb}}{G_{mm}}\right)$$

2. $$VMA = 100 - \frac{G_{mb} \times P_s}{G_{sb}}$$

3. $$VFA = 100 \times \left(\frac{VMA - VTM}{VMA}\right)$$

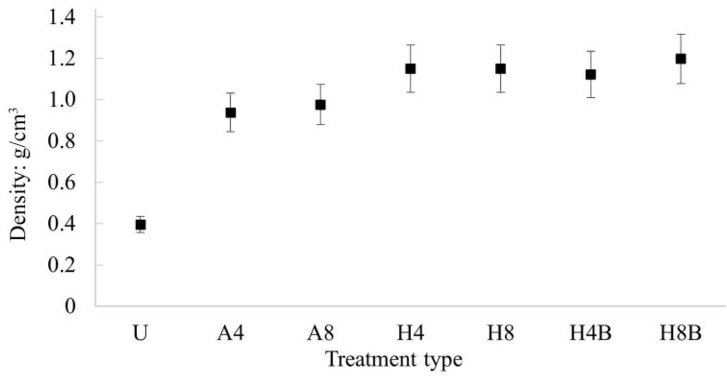

Figure 5. Measured density of untreated and treated fibres

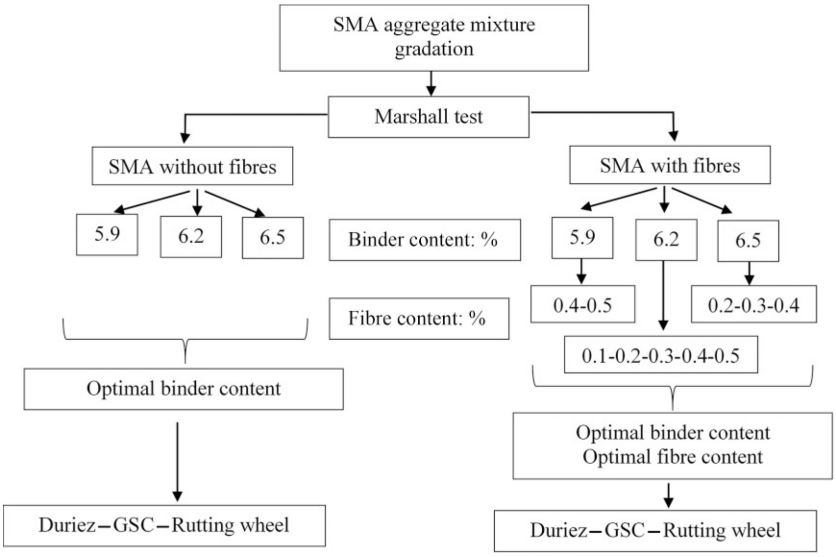

Figure 6. Experimental programme flowchart

4. $$VCA_{DRC} = 100 \times \left(\frac{G_{ca} Y_w - Y_s}{G_{ca} Y_s} \right)$$

5. $$VCA_{mix} = 100 - \frac{G_{mb}}{G_{ca}} P_{ca}$$

2.3.2 Duriez test

The Duriez test followed the European standard EN 12697-12 (ESC, 2018). For each mix, eight specimens were prepared using 80 mm-diameter moulds preheated for 4 h at 155°C and compacted using a static force of 60 kN. Three specimens were stored in air and three in water at 18°C for 7 days, and two specimens were used for density measurements. After this period, the six specimens underwent uniaxial compression at a constant rate of 1 mm/s, yielding the strength of specimens preserved in the air, denoted by *R*, and the strength of specimens preserved in water, denoted by *r*. The ratio *r/R*, referred to as the immersion/compression ratio, reflects the sensitivity of the HMA mixture to moisture. The compressive strength, *R*, was also used in this study as an indicator of performance. Even though the test is applied in compression, it is also an indicator of shear strength.

2.3.3 Gyratory shear compactor test

The GSC test was performed according to the EN 12697-31 standard (ESC, 2019). Two specimens per mix were compacted using a gyration angle of 1° and a constant vertical pressure of 600 kPa using 150 mm-diameter moulds at a temperature of 155°C. The machine records the specimen height with the number of gyrations. The height data are then used to calculate the degree of compaction relative to the maximum theoretical density of the mixture. Mixes that compact too quickly (high degree of compaction at a low number of gyrations) may be tender during construction and unstable when subjected to traffic.

2.3.4 Rutting wheel test

This test followed the European standard EN 12697-22 (ESC, 2020b). Two slabs measuring 500 × 180 mm × 100 mm^3 for each tested mixture were prepared at an air void content of 6%. After settling for 3 days to provide sufficient time for the bituminous binder to adhere to the aggregate particles, each pair of slabs underwent rutting wheel testing. In this test, a single pneumatic (width 80/62.5/R200) tyre with a load of 5 kN and a pressure of 600 kPa moves on top of the HMA slab on the same path in a back-and-forth motion at a frequency of 1 Hz. The testing temperature is set at 60°C. The rut thickness is automatically measured at 1000, 3000, 10 000, and 30 000 cycles.

3. Results and discussion

As mentioned earlier, the main step of the SMA formulation is the establishment of a gradation curve for the aggregate mixture based on an NMAS. Since the NMAS used for dense-graded mixtures in the country is 14 mm, the decision was to use an existing recommended gradation for an SMA mix with an NMAS close to 14 mm. After several trials with the USA, Europe, and Asia recommendations for SMA, 12.5, 13, and 11 mm, respectively, the only guidelines met by the classes of aggregates selected for the study were those of the Indian Road Congress for SMA 13. The percentage of the aggregate classes was 12% class 0/4, 0% class 4/8, 77% class 8/16, and 11% filler. The mixture gradation, as well as the upper and lower bounds, is shown in Figure 7.

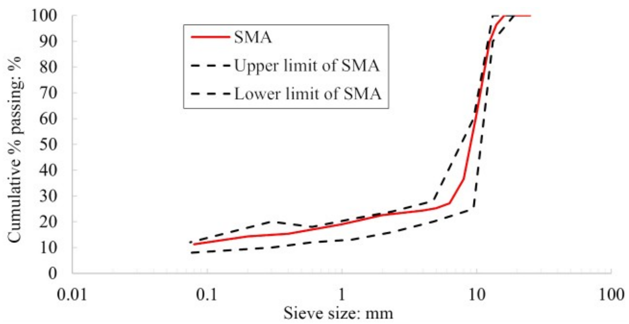

Figure 7. SMA 13 aggregates' mixture gradation

Once the mixture gradation was established, the next step was to determine the optimum % asphalt for the SMA without fibres and the optimum % bitumen and optimum % fibres for the SMA with fibres. This task was achieved using the Marshall results as outlined in the Section 3.1 Marshall test results.

3.1 Marshall test results

Table 3 displays the results of all performed Marshall method tests, volumetric properties, and the standard deviation is shown between parentheses for all 13 evaluated SMA mixtures (three without fibres and ten with fibres). The optimal asphalt content (OAC) for SMA without fibres was found to be 6.2%, achieving a VTM of 4% air voids, a VMA of 17.8%, and a VFA of 77%, and the highest stability value of 4.9 kN, which is lower than the specified value of 6.2 kN. On the contrary, SMA mixtures incorporating cellulose fibres exhibited higher VTM values compared with those without fibres. The OAC for SMA mixtures with fibres was determined to be 6.5%, with a treated Juncus fibre content of 0.4%. This mixture had the exact specified value of 4% for the VTM, a stability of 5.7 kN, a flow of 3.4 mm, a VMA of 18.6, and a VFA of 78.6%. Therefore, all the criteria were met for this mixture, except for the stability property, which was found to be a bit lower than the specified value of 6.2 kN. The general trend found from all these Marshall tests is that fibres tend to increase the binder content and the VTM, but with a noticeable improvement in stability. This demonstrates the effect of fibres on SMA performance not only in terms of draindown but also in terms of shear resistance.

Once the retained formulas for SMA with and without fibres were developed (shaded in grey in Table 3), the following step was to evaluate the performance of these two mixtures against rutting, which will be discussed in the Section from 3.2 to 3.4.

3.2 Duriez test results

Figure 8 presents the results of the compressive strength test performed at 18°C, known as the Duriez test. Even though the results of this test are used to assess the moisture susceptibility of an HMA mixture, it could be used to compare the resistances, which are an indirect indication of shear strength at the testing temperature. Both mixtures passed the criterion of resistance to moisture attack, as the ratio of the average of water-stored specimens' strength to that of the air-stored ones is equal to 0.88 and 0.86 for the SMA with fibres and SMA without fibres, respectively. These ratios are higher than the limiting value of 0.8. However, looking into the average compressive strength itself, it is noticed that the SMA with fibres exhibited higher values. The average strength of the three air-stored specimens for SMA without fibres was equal to 6.5 MPa, while that of the SMA with fibres was higher by about 1.7 times (11.3 MPa). Even though the temperature of this test is 18°C, which is not a temperature when rutting might occur but using the time-temperature superposition principle, pavements with slow-moving trucks might be in danger of such a defect even

Table 3. Results of the Marshall design method for the 13 evaluated SMA mixtures

Asphalt: %	Fibre: %	Stability: kN	Flow: mm	VTM	VMA	VFA	VCA_{DRC}	VCA_{mix}
SMA without fibres								
5.9	0	4.5 (0.4)	3.2 (0.3)	5.8 (0.2)	18.7	69	47.2	40.5
6.2	0	4.9 (0.2)	3.3 (0.1)	4 (0.4)	17.8	77	47.2	39.9
6.5	0	4.5 (0.4)	3.7 (0.1)	3.1 (0.02)	17.5	82	47.2	39.6
SMA with fibres								
5.9	0.4	5.1 (0.6)	3.6 (0.6)	6 (0.5)	19.4	69.3	47.2	41.2
	0.5	4.6 (0.4)	5.0 (0.4)	6.1 (0.3)	19.7	69.0	47.2	41.5
6.2	0.1	6.0 (0.3)	3.2 (0.2)	4.1 (0.2)	17.9	77.0	47.2	40.1
	0.2	5.7 (0.2)	3.1 (0.1)	4.2 (0.6)	18.1	76.8	47.2	40.2
	0.3	5.6 (0.7)	3.4 (0.6)	4.3 (0.4)	18.4	76.7	47.2	40.4
	0.4	4.3 (0.5)	3.4 (0.5)	4.4 (0.2)	18.6	76.6	47.2	40.5
	0.5	4.3 (0.6)	3.8 (0.5)	4.5 (0.6)	18.9	76.4	47.2	40.6
6.5	0.2	4.5 (0.1)	3.2 (0.4)	3.9 (0.7)	18.5	78.8	47.2	40.5
	0.3	5.5 (0.1)	3.3 (0.2)	3.9 (0.7)	18.6	78.8	47.2	40.6
	0.4	5.7 (0.5)	3.4 (0.1)	4 (0.4)	18.7	78.6	47.2	40.7
Specs.	**—**	**≥6.2**	**24**	**4**	**>17**	**7090**	**$VCA_{mix} < VCA_{DRC}$**	

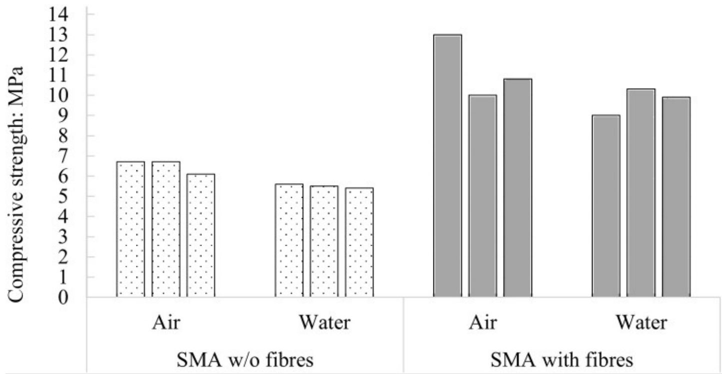

Figure 8. Duriez compressive strength at 18°C for all SMA specimens

at this low temperature. In addition, pavement areas with shearing forces (acceleration/deceleration and roundabouts) might exhibit such a defect even at this low temperature. Therefore, the fibres show an improvement in the performance of SMA to flow rutting even at this low temperature of 18°C.

3.3 Gyratory shear compactor test results

Figure 9 displays the results of the GSC tests performed on SMA with and without fibres. The figure shows the average degree of compaction of the two tests performed per mixture. The difference between the readings on the same mixture was smaller than 2%, which indicates good repeatability of the test and led to the analysis of the average results without consideration of the within errors. Both mixtures showed good resistance to compaction at early gyrations as they verified the criterion indicating tender mixes, which is a degree of compaction smaller than 89% at 10 gyrations. The SMA without fibres showed stronger resistance, as the degree of compaction at 10 gyrations was 81.6%, while that for the SMA with fibres was 82.9%. However, after about 100 gyrations, the trend was reversed, and the SMA with fibre mix started to show more resistance to compaction. For instance, at 200 gyrations, the degree of compacity was calculated as 98.5 and 99.5 for the SMA with fibres and without fibres, respectively. This could be explained by the fact that fibres tend, at the start of the compaction, to be part of the HMA matrix and therefore do not resist compaction. Once the fibres are part of the HMA matrix, they increase the shear resistance of the mix. This trend is also shown by the excellent fit (coefficient of determination, R^2, higher than 0.99) established using power regression equations relating the degree of compaction (variable y) to the number of gyrations (variable x), shown in Figure 9. The initial rate of compaction is higher for SMA with fibres (72.7% for 1 gyration), but the rate of compaction is slower for this mix (exponent of 0.0577).

3.4 Rutting wheel test results

Figure 10 shows the rutting wheel test results for both specimens of the tested SMA mixtures. The plotted graphs show the measured rut in mm as a function of loading cycles (a cycle is a back-and-forth movement). For each mix, the results of both specimens are shown as well as their averages to quantify the

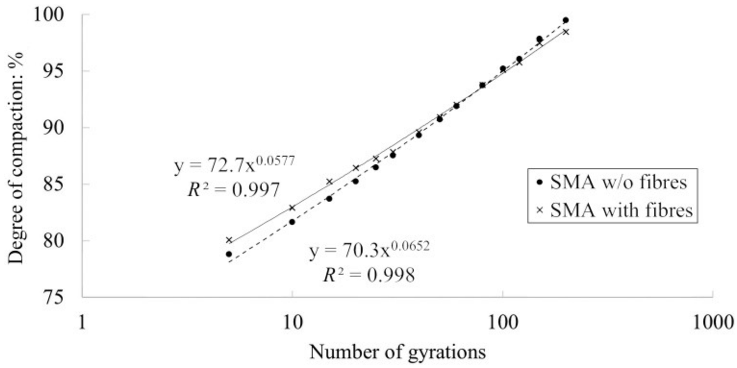

Figure 9. GSC average test results for SMA with and without fibres

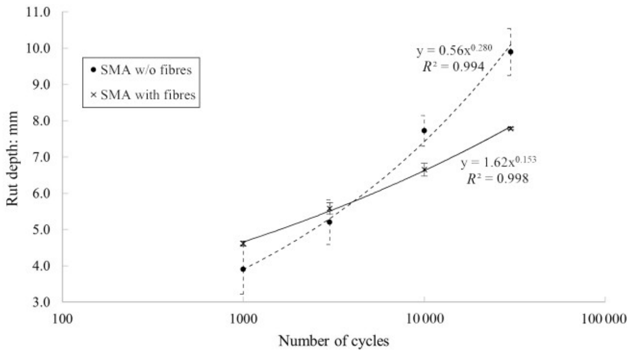

Figure 10. Rutting wheel test results for SMA with and without fibres

within-group variability. The highest within-mix variability was found at low cycle numbers for the SMA without a fibre mixture. A variability as high as 29.7% and 21.1% was calculated at 1000 and 3000 cycles, respectively. For a higher number of cycles, this variability dropped to less than 12.2%. The SMA mix with fibres showed lesser variability, as the highest observed difference between two measurements was 5.4% at 3000 cycles. The trend found with the GSC test results was repeated with the rutting wheel test results. In fact, at early loading cycles, the measured rut depth is higher for the SMA with a fibre mixture. This can be attributed to initial compaction and slight rearrangement of the mix structure due to the presence of fibres. Then at about 4400 cycles, the behaviour is reversed, and the measured rut depth becomes smaller than that measured for the SMA without a fibre mixture. For instance, at 30 000 cycles, the average measured rut depth for the SMA with fibres was 7.8 mm, which represents about 79% of the average rut depth for the SMA without fibres (9.9 mm). This trend is quantified using the power regression equations ($R^2 > 0.99$) established for both mixtures and is shown in Figure 10. The initial rut depth (after one cycle) for the SMA without fibres is equal to 0.56 mm, which is less than that for the SMA with fibres (1.62 mm). However, the rut developed, as quantified with the power exponent, is much higher for the SMA without fibres than that for the SMA with fibres (0.28 against 0.153). In summary, at 30 000 cycles, the SMA with a fibre mixture showed much less rut depth (average of 7.8 mm) and much less variability between the two tested slabs (0.9%), as compared with its counterpart without fibre (average rut depth of 9.9 mm and 12.2% variability). These results confirm that the fibres play a crucial role in interlocking with HMA particles to enhance cohesion under wheel loads, thereby increasing shear resistance and structural uniformity, which significantly improves rutting resistance.

4. Conclusions and recommendations for future research

The main goal of this research was to formulate an SMA mixture based on the Marshall design method using locally available materials. For that reason, the research started by looking into a local source for natural fibres used as a stabiliser in SMA production. The important aspects of the study are summarised as follows:

(*a*) The Juncus plant was found to be a suitable source for cellulose fibres following a chemical treatment. The optimal type of treatment fulfilling the project's objective was selected as 1-h hot treatment at 98°C using 8% sodium hydroxide, followed by 1 h in sodium hypochlorite, producing fibres with suitable properties in terms of cellulose content (64%), yield, and morphology.
(*b*) Based on Marshall tests, extracted cellulose fibres were found to increase the total voids of the mixture and the OAC.
(*c*) The Duriez test performed at 18°C demonstrated an increase in compressive strength, which correlates with shear resistance, by the incorporation of fibres. At this intermediate temperature, the increase in shear strength is important for areas with slow-moving trucks, acceleration and deceleration zones, and roundabouts.
(*d*) Shear gyratory compaction tests at 155°C led to the conclusion that fibres take time to be part of the structural matrix of the mix, then play an important role in increasing the shear strength and therefore the energy of compaction.
(*e*) The rutting wheel test performed at 60°C showed that cellulose fibres extracted from the Juncus plant significantly increase the resistance of SMA against rutting. The fibre-reinforced SMA mixture showed a 21% reduction in rut depth compared with the mixture without fibres and exhibited slower rut progression under repeated loading.

Given the limited number of specimens (two per mixture) performed during this study, the following tasks are recommended for future research:

(*a*) More testing of extracted fibres, such as oil absorption and pH.
(*b*) Use of other sources of aggregates to match SMA gradations as recommended by other agencies in the USA and Europe.
(*c*) For each performed test, at least six specimens per designed mixture should be evaluated in order to obtain better statistically confident results.
(*d*) For the wheel tracking tests, slabs prepared initially at a 4% VTM should be evaluated.
(*e*) In this study, 35–50 penetration-graded virgin asphalt was used because of the local highway agency requirements; future investigation with polymer-modified asphalt is recommended. The addition to the initial production cost could be more than justified by the increased performance against rutting, especially since the country is moving towards more road transportation, and the weather is getting hotter due to climate change. However, a detailed life cycle cost analysis is recommended.

Acknowledgements

The authors gratefully acknowledge the scientific collaboration of Dr. Khiari with the cellulose fibres' testing. And the director of the Centre for Testing and Construction Techniques-Tunis Mohamed Guesmi, for his guidance in letting us do all the mechanical tests of the asphalt mixture.

REFERENCES

AASHTO (American Association of State Highways and Transportation Officials) (2023) Standard No. M320, Standard Specification for Performance Graded Asphalt Binder. AASHTO, Washington, DC, USA.

AFNOR (French Standardisation Association) (1985) Standard No. NF T20-053: Chemical Products for Industrial Use – Determination of the Density of Powdered Solids and Liquids – Pycnometer Method. AFNOR, Paris, France.

AFNOR (2001) NF EN 1097-6, Tests for Mechanical and Physical Properties of Aggregates – Part 6: Determination of Particle Density and Water Absorption. AFNOR, Paris, France.

AFNOR (2011) NF EN 1097-1: Tests for Mechanical and Physical Properties of Aggregates – Part 1: Determination of the Resistance to Wear (micro-Deval). AFNOR, Paris, France.

AFNOR (2012) NF EN 933-3: Tests for Geometrical Properties of Aggregates – Part 3: Determination of Particle Shape – Flakiness Index. AFNOR, Paris, France.

AFNOR (2015a) NF EN 1426: Bitumen and Bituminous Binders – Determination of Needle Penetration. AFNOR, Paris, France.

AFNOR (2015b) NF EN 1427: Bitumen and Bituminous Binders – Determination of the Softening Point – Ring and Ball Method. AFNOR, Paris, France.

AFNOR (2015c) NF EN 933-8: Tests for Geometrical Properties of Aggregates - Part 8: Assessment of Fines – Sand Equivalent Test. AFNOR, Paris, France.

AFNOR (2020) NF EN 1097-2: Tests for Mechanical and Physical Properties of Aggregates – Part 2: Methods for the Determination of Resistance to Fragmentation. AFNOR, Paris, France.

Ben Dhia T, Loulizi A, Hofko B and Kammoun AA (2024) Quantifying ageing of 35-50 and 70-100 asphalts using Fourier transform infrared spectroscopy and dynamic shear rheometer measurements. *International Journal of Engineering Research in Africa* **68**: 99–115.

Blazejowski, K (2011) *Stone Matrix Asphalt-Theory and Practice*, CRC Press Taylor & Francis Group, Boca Raton, London, New York.

Brown ER, Cooley LA, Haddock JE, Hughes CS and Lynn TA (1998). *Designing Stone Matrix Asphalt Mixtures Volume IV – Mixture Design Method, Construction Guidelines, and Quality Control Procedures*. National Centre for Asphalt Technology.

Brown ER, Haddock JE, Mallick RB and Lynn TA (1997a). *Development of a Mixture Design Procedure for Stone Matrix Asphalt (SMA)*. National Center for Asphalt Technology.

Brown ER, Mallick RB, Haddock JE and Bukowski J (1997b) Performance of stone matrix asphalt (SMA) mixtures in the United States. *Journal of the Association of Asphalt Paving Technologists* **66**.

El Ghali A, Ben Marzoug I, Baouab MH and Roudesli MS (2012) Separation and characterization of new cellulosic fibres from the *Juncus acutus* L plant. *BioResources* **7(2)**: 2002–2018.

ESC (European Committee for Standardization) (2014) EN 12607-1: Bitumen and Bituminous Binders Determination of the Resistance to Hardening under Influence of Heat and Air Part 1: RTFOT Method.

ESC (2017) EN ISO 2592: Petroleum and Related Products Determination of Flash and Fire Points Cleveland Open Cup Method.

ESC (2018) EN 12697-12: Bituminous Mixtures Test Methods – Part 12: Determination of the Water Sensitivity of Bituminous Specimens.

ESC (2019) EN 12697-31: Bituminous Mixtures – Test Methods – Part 31: Specimen Preparation by Gyratory Compactor.

ESC (2020a) EN 12697-34: Bituminous Mixtures – Test Methods – Part 34: Marshall Test.

ESC (2020b) EN 12697-22: Bituminous Mixtures Test Methods Part 22: Wheel Tracking.

Jasni NE, Masri KA, Ramadhanhansyah PJ, *et al.* (2020) Mechanical performance of stone mastic asphalt incorporating steel fibre. *IOP Conference Series: Materials Science and Engineering*, 10.1088/1757-899X/712/1/012026.

Mokhtari A and Nejad FM (2012) Mechanistic approach for fibre and polymer modified SMA mixtures. *Construction and Building Materials* **36**: 381–390, 10.1016/j.conbuildmat.2012.05.032.

Naili H, Jelidi A, Limam O and Khiari R (2017) Extraction process optimization of Juncus plant fibres for its use in a green composite. *Industrial Crops and Products* **107**: 172–183.

NAPA (National Asphalt Pavement Association) (2002) *Designing and Constructing SMA Mixtures: State of the Practice Quality Improvement Series 122*. NAPA, Lanham, MD, USA.

NCHRP (National Cooperative Highway Research Program) (1999) *Designing Stone Matrix Asphalt Mixtures for Rut-Resistant Pavements, Report 425*. National Academy Press, Washington DC, USA.

Omrani H, Hassini L, Benazzouk H, Beji H and ElCafsi A (2020) Elaboration and characterization of clay-sand composite based on *Juncus acutus* fibres. *Construction and Building Materials* **238**: 117712, 10.1016/j.conbuildmat.2019.117712.

Raghuram KB and Chowdary V (2013) Performance evaluation of stone matrix asphalt (SMA) using low-cost fibres. *Journal of the Indian Roads Congress* **74(2)**: 159–174.

Simms R, Hernando D and Roque R (2020) A new paradigm to explain the development of instability rutting in asphalt pavements. *Road Materials and Pavement Design* **21(7)**: 1815–1828, 10.1080/14680629.2019.1568286.

TAPPI (Technical Association of the Pulp and Paper Industry) (1991) *No. um 250-91, "Acid-Soluble Lignin in Wood and Pulp"*. TAPPI Press, Atlanta, GA, USA.

TAPPI (1999) *No. T203 cm-99, "Alpha-, Beta- and Gamma-Cellulose in Pulp"*. TAPPI Press, Atlanta, GA, USA.

TAPPI (2006) *No. T222 om-06, "Acid-Insoluble Lignin in Wood and Pulp"*. TAPPI Press, Atlanta, GA, USA.

TAPPI (2007) *No. T211 om-07, "Ash in Wood, Pulp, Paper and Paperboard: Combustion at 525°C"*. TAPPI Press, Atlanta, GA, USA.

Wise LE, Murphy M and D'Addieco AA (1946) Chlorite holocellulose: its fractionation and bearing on summative wood analysis and on studies on the hemicellulose. *Paper Trade Journal* **122(2)**: 35–43.

Yin F and West RC (2018) *Performance and Life-Cycle Cost Benefits of Stone Matrix Asphalt Report No. 18-03*. National Center for Asphalt Technology.

How can you contribute?

To discuss this paper, please email up to 500 words to the editor at support@emerald.com. Your contribution will be forwarded to the author(s) for a reply and, if considered appropriate by the editorial board, it will be published as discussion in a future issue of the journal.

Proceedings journals rely entirely on contributions from the civil engineering profession (and allied disciplines). Information about how to submit your paper online is available at www.emeraldgrouppublishing.com/journal/jcoma, where you will also find detailed author guidelines.